A&A 380, 471–477 (2001)
DOI: 10.1051/0004-6361:20011486

Astronomy & Astrophysics

The fundamental plane of radio galaxies⋆

D. Bettoni[1], R. Falomo[1], G. Fasano[1], F. Govoni[2], M. Salvo[1], and R. Scarpa[3]

[1] Osservatorio Astronomico di Padova, Vicolo Osservatorio 5, 35122 Padova, Italy
e-mail: falomo@pd.astro.it; fasano@pd.astro.it; salvo@pd.astro.it
[2] Istituto di Radioastronomia di Bologna and Dipartimento di Astronomia, Universitá di Bologna, Italy
e-mail: fgovoni@ira.bo.cnr.it
[3] European Southern Observatory
e-mail: rscarpa@eso.org

Received 10 September 2001 / Accepted 15 October 2001

Abstract. We collected photometrical and dynamical data for 73 low red-shift ($z < 0.2$) Radio Galaxies (LzRG) in order to study their Fundamental Plane (FP). For 22 sources we also present new velocity dispersion data that complement the photometric data given in our previous study of LzRG (Govoni et al. 2000a). It is found that the FP of LzRG is similar to the one defined by non-active elliptical galaxies, with LzRG representing the brightest end of the population of early type galaxies. Since the FP mainly reflects the virial equilibrium condition, our result implies that the global properties of early–type galaxies (defining the FP) are not influenced by the presence of gas accretion in the central black hole. This is fully in agreement with the recent results in black hole demography, showing that virtually all luminous spheroidal galaxies host a massive black hole and therefore may potentially become active. We confirm and extend to giant ellipticals the systematic increase of the mass-to-light ratio with galaxy luminosity.

Key words. galaxies: general

1. Introduction

It is well known that the global properties of early–type galaxies are fairly well described through a three dimensional space of observables which, besides the effective radius r_e and the corresponding average surface brightness $<\mu_e>$, involves the central velocity dispersion σ_c (Djorgovski & Davis 1987; Dressler et al. 1987). In fact, ellipticals and lenticulars are found to lie in a surprisingly tight, linear region of this space (the so called Fundamental Plane; hereafter FP) that has been shown to be close to the plane defining the virial equilibrium condition over the assumption of a rigorous homology among galaxies (Faber et al. 1989).

The systematic deviation of the FP from the one defined by the virial equilibrium, has been interpreted as due to changes of the Mass to Light ratio (M/L) (due to different stellar content or to differences in dark matter distribution; Pahre et al. 1995; Mobasher et al. 1999), as well as to the breakdown of the homology assumption (e.g. kinematic anisotropy; Caon et al. 1993; Graham et al. 1996; Ciotti et al. 1996; Busarello et al. 1997). In this context it is therefore important to determine whether the FP has universal validity among ellipticals. In particular it is not yet clear if active and non-active galaxies do follow the same FP, as it would be expected in view of the recent results on Black Holes (BH) demography in galaxies (Gebhardt et al. 2000; Ferrarese & Merritt 2000).

A relevant case is that of low redshift extragalactic radio sources that are associated with massive early–type galaxies. A number of optical studies have been carried out in the last decade to investigate the relationship between radio emission properties and the characteristics of the host galaxies (see e.g. Govoni et al. 2000a and references therein). Comparison of the optical properties of radio galaxies with those of normal (non radio) ellipticals have shown that the probability to exhibit radio emission increases with the optical luminosity of the galaxies (Scarpa & Urry 2001) and also that the radio morphology (typically classes FR I and FR II) may depend on the absolute magnitude of the host galaxy (Owen & Laing 1989; Owen & White 1991). This could be related to the different BH mass (proportional to the galaxy luminosity) and to the jet power (Ghisellini & Celotti 2001).

As a whole, these studies have shown that the optical morphological/structural and photometrical properties of radio and non-radio ellipticals are remarkably similar, suggesting that all ellipticals may go through a phase of

Send offprint requests to: D. Bettoni,
e-mail: bettoni@pd.astro.it

⋆ Based on observations collected at European Southern Observatory, La Silla, Chile.

nuclear activity lasting for a small fraction of the total life of the galaxy.

Few previous observations were devoted to investigation of the dynamical properties of Radio Galaxies (RG). Apart a very small number (11) of radio sources included in the original work on the FP of ellipticals by Faber et al. (1989) (hereafter FA89), only Smith et al. (1990; hereafter SHI90) performed a systematic study on the stellar dynamics of Powerful Radio Galaxies (PRG). They compared $<\mu_e>$, r_e and σ_c measurements for a compilation of PRG with the distribution in the FP of the bright ellipticals studied by FA89, concluding that the FP of PRG is consistent with that of normal ellipticals. However they also found evidence for smaller than normal velocity dispersions and significant rotational support in galaxies with marked morphological peculiarities.

In this paper we present a much deeper investigation of the FP of radio galaxies, based on a sample of 73 radio galaxies. The data are in part new (22 objects) and in part collected from the literature (51 objects). Most of literature values were derived from the Hypercat database (Prugniel & Maubon 2000). All values of $<\mu_e>$, r_e, and σ_c have been processed in order to make them homogeneous to a common standard (see Sect. 4.2). Throughout the paper we assume $H_0 = 50\ h^{-1}$ km s^{-1} Mpc^{-1} and $q_0 = 0$.

Table 1. Log of the observations.

Object	α (2000)	δ (2000)	z	Exptime s	PA[a]
0055–016	00 57 35	−01 23 28	0.045	4800	90
0131–360	01 33 58	−36 29 35	0.030	3600	90
0257–398	02 59 27	−39 40 37	0.066	4800	120
0312–343	03 14 33	−34 07 40	0.067	3600	145
0325+024	03 27 54	+02 33 42	0.030	3600	155
0449–175	04 51 21	−17 30 14	0.031	3600	180
0546–329	05 58 27	−32 58 37	0.037	3000	180
0548–317	05 50 49	−31 44 26	0.034	3600	180
0718–340	07 20 47	−34 07 05	0.029	7200	75
0915–118	09 18 06	−12 05 43	0.054	4800	43
0940–304	09 42 23	−30 44 11	0.038	7200	87
1043–290	10 46 10	−29 21 10	0.060	7200	180
1107–372	11 09 57	−37 32 17	0.010	3600	32
1123–351	11 25 53	−35 23 40	0.032	6000	85
1251–122	12 54 40	−29 13 39	0.015	3600	17
1333–337	13 36 39	−33 57 56	0.013	3600	60
1400–337	14 03 39	−33 58 43	0.014	3600	84
1404–267	14 07 29	−27 01 02	0.022	4800	105
1514+072	15 16 45	+07 01 17	0.035	4800	5
1521–300	15 24 33	−30 12 20	0.020	5400	60
2236–176	22 39 11	−17 20 28	0.070	4800	124
2333–327	23 36 07	−32 30 30	0.052	4800	173

[a] Slit position angle in degrees from North toward East.

2. Observations and data analysis

We obtained medium resolution optical spectra of RG selected from the brightest ($m_R < 15$) objects in the sample of 79 LzRG previously imaged, in the R filter, by us (Fasano et al. 1996; Govoni et al. 2000a,b). These observations were aimed at deriving the velocity dispersion from stellar absorption lines. In Table 1 we give the list of the objects observed together with exposure times and position angles used for the observations.

Optical spectroscopy was obtained in March/April 1998 and November 1998 with the ESO/Danish 1.52 m telescope at La Silla, using the Danish Faint Object Spectrograph and Camera (DFOSC). We used a CCD Loral/Lesser, with 2052 × 2052 pixels combined with an Echelle Grism of 316 grooves/mm yielding a velocity resolution ($FWHM$) of 71 km s^{-1} (for a slit 1″ wide) in the range $\lambda\lambda = 4800-5800$ Å. A long slit, 2.0″ wide and centered on the galaxy, was oriented along the apparent major axis of the radio galaxy. With this configuration we reach a velocity dispersion resolution $\Delta\sigma = 60$ km s^{-1}; the scale perpendicular to the dispersion is 0.39″/pixel. Template reference spectra of standard stars of spectral type from G8-III to K1-III, with low rotational velocity ($V \times \sin(i) < 17$ km s^{-1}), were secured at the beginning and at the end of each night. During the observations the seeing ranged between 1″ and 1.5″.

Optical spectra were reduced using standard procedures available in the IRAF package and includes bias subtraction, flat fielding, and wavelength calibration. The accuracy of the latter procedure was checked with measurements of the night sky $\lambda_0 = 5577.32$ Å emission line. In all cases a precision of $\lesssim$20 km s^{-1} was reached. In order to increase the signal to noise and to match the observed spatial resolution (assuming the mean seeing) with the plate scale across dispersion, the spectra were rebinned over three pixels perpendicular to the dispersion, obtaining an effective spatial resolution of 1.17″/pixel. The observed spectral range includes the Mg_2 band ($\lambda_0 =$ 5175.4 Å), the E-band (5269 Å) and the FeI line (5335 Å).

The systemic velocity, corrected to the Sun, and the velocity dispersion σ were determined using the Fourier Quotient method (Sargent et al. 1977; Bertola et al. 1984). The spectra were first normalized by subtracting the continuum, converted to a logarithmic scale and then multiplied to a cosine bell function that apodizes 10% of the pixels at each end of the spectrum. This forces the ends of the spectra smoothly to zero. Finally the Fourier Transform of the galaxy spectra were divided by the Fourier Transform of a template star whose spectra (late G and early K spectral type) matched that of the galaxy. These spectra are used as templates of zero velocity dispersion.

The best-fit stellar template then yields a profile of the velocity dispersion σ and the stellar velocity curve with relative errors for the galaxy. The rms of the determinations obtained with different template stars turned out to be less than 20 km s^{-1} for σ and ∼10 km s^{-1} for the systemic radial velocity V_r. The average values of these determinations were adopted as final values of σ and V_r.

Since early-type galaxies exhibit some gradients in the radial velocity and velocity dispersion (Davies et al. 1983; Fisher 1995), the derived "central" parameter σ_c depends

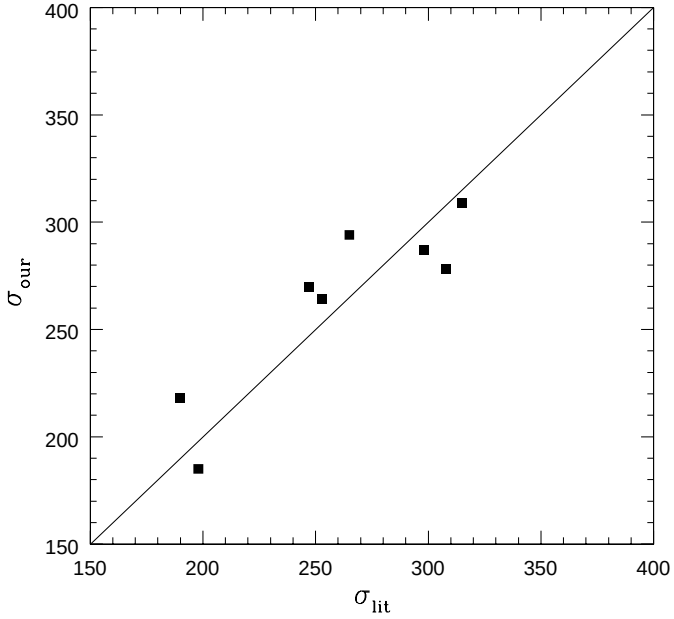

Fig. 1. Our velocity dispersion σ measurements compared with the literature data.

on the distances of the galaxies and the size of the aperture used for the observation. In order to compare our velocity dispersions with the data available in the literature we applied aperture corrections according to the procedure given by Jørgensen et al. (1995). The individual measurements of σ are therefore corrected to a circular aperture with a metric diameter of $1.19\,h^{-1}$ kpc , equivalent to $3.4''$ at the distance of the Coma cluster.

For 8 of the 22 RGs observed previous determinations of the velocity dispersion were found in the Hypercat database. The comparison between our and previous measurements of σ is shown in Fig. 1. When more than one measurement of σ is present in the literature, we took the mean value quoted by Hypercat. The average difference between our and Hypercat values of σ is:

$$< \sigma_{\rm our} - \sigma_{\rm Hyp} > = 4 \pm 6.4 \ {\rm km\,s^{-1}}; \quad {\rm rms} = 18 \ {\rm km\,s^{-1}}.$$

Additional notes on individual galaxies are given in the Appendix.

Table 2 reports our measurements of $\sigma_{\rm c}$ and the estimated uncertainities, together with the parameters $<\mu_{\rm e}>$ and $r_{\rm e}$, taken from Govoni et al. (2000a), that are relevant to construct the FP. The average surface brightness $<\mu_{\rm e}>$ has been evaluated from the formula:

$$<\mu_{\rm e}> = R_{\rm T} + 5 \ \log(r''_{\rm e}) + 2.5 \ \log(2\pi),$$

where $R_{\rm T}$ is the total R apparent magnitude and $r''_{\rm e}$ is the effective radius. All these quantities are corrected for the contribution of the point source (see Govoni et al. 2000b), for cosmological dimming and for K–correction according to Poggianti (1997). The distance/systemic velocities used to derive $r_{\rm e}$ and $<\mu_{\rm e}>$ are relative to the Cosmic Microwave Background (CMB) reference frame and come from the Lyon Meudon Extragalactic Database (LEDA, Paturel et al. 1997).

Table 2. Photometrical and kinematical Data for our sample of radio galaxies.

name	$<\mu_{\rm e}>$	$\log r_{\rm e}$ kpc	$\log\sigma$ km s^{-1}	$\Delta\log\sigma$	$V_{\rm r}$ km s^{-1}
0055–016	19.98	1.102	2.48	0.11	13 593
0131–360	20.16	1.145	2.40	0.17	8771
0257–398	19.25	0.872	2.34	0.16	19 814
0312–343	21.25	1.352	2.41	0.07	20 516
0325+024	21.46	1.301	2.34	0.12	9875
0449–175	20.50	1.163	2.20	0.15	9548
0546–329	20.47	1.267	2.59	0.34	11 100
0548–317	20.34	0.988	2.09	0.48	10 352
0718–340	19.70	1.043	2.52	0.50	9578
0915–118	20.90	1.342	2.44	0.07	16 171
0940–304	19.72	0.973	2.59	0.20	12 610
1043–290	21.80	1.572	2.36	0.18	19 527
1107–372	19.66	1.093	2.47	0.09	3362
1123–351	20.95	1.382	2.65	0.84	10 632
1258–321	20.40	1.237	2.42	0.12	5553
1333–337	19.76	1.139	2.46	0.56	4122
1400–337	20.70	1.408	2.49	0.20	4567
1404–267	20.70	1.210	2.47	0.06	7187
1514+072	21.89	1.620	2.43	0.12	11 130
1521–300	19.60	0.563	2.22	0.02	6579
2236–176	21.33	1.492	2.39	0.15	22 396
2333–327	19.86	1.022	2.43	0.03	15 707

3. Extended sample of LzRG

We have collected from the literature stellar velocity dispersion measurements of LzRGs for which photometric and structural parameters are also available. To make these data homogenous with our measurements we processed them applying the same procedure adopted for our subsample of LzRG (see above section and Govoni et al. 2000b).

We excluded from the analysis the radio galaxies belonging to dumbbell systems or close galaxy pairs, as well as those having recession velocity (corrected to CMB) less than 3000 km s^{-1}, since these circumstances may induce significant uncertainties in the parameters considered.

3.1. Previous work on the Fundamental Plane of LzRGs

An early investigation of the FP of LzRG was undertaken by FA89 in their study of early-type galaxies. They give $<\mu_{\rm e}>$ and $r_{\rm e}$ (in the B band), as well as σ for 11 RGs. However 6 objects are dumbbell systems or have small recession velocity and for this reason are not considered in our analysis. For the remaining 5 we obtained $<\mu_{\rm e}>$ in the R band applying a color correction based on the integrated color $(B-R)$ obtained from Hypercat.

The first systematic study of the FP of RGs was performed by Smith et al. (1990, SHI90) who reported kinematical and photometrical data for 20 powerful radio galaxies previously imaged in the V band (Smith & Heckman 1989, hereafter SH89), as well as for 16 more

Table 3. Radio Galaxies from literature.

name	$\log\sigma$ $\mathrm{km\,s^{-1}}$	$\log r_\mathrm{e}$ kpc	$<\mu_\mathrm{e}>$	V_r $\mathrm{km\,s^{-1}}$
Smith et al. (1990)				
3C 29	2.318	1.075	21.25	13 400
3C 31	2.394	1.522	21.27	5007
3C 33	2.362	0.841	21.43	17 840
3C 62	2.436	0.637	22.92	44 370
3C 76.1	2.301	0.816	20.93	9713
3C 78	2.417	1.182	20.99	8634
3C 84	2.391	1.532	20.96	5156
3C 88	2.276	1.434	22.61	9054
3C 89	2.398	1.007	23.37	41 550
3C 98	2.238	1.081	21.32	9174
3C 120	2.301	1.165	21.14	10 010
3C 192	2.283	0.691	21.31	17 930
3C 196	2.322	0.707	23.00	59 360
3C 223	2.305	0.593	22.06	41 010
3C 293	2.267	0.750	21.27	13 550
3C 305	2.250	0.658	19.56	12 470
3C 338	2.462	1.616	21.91	9084
3C 388	2.562	1.220	22.55	27 220
3C 444	2.190	1.117	23.58	45 870
3C 449	2.350	1.754	22.77	5126
PKS 0634–206	2.290	0.660	19.80	16 790
PKS 2322–122	2.350	1.103	22.55	24 610
Faber et al. (1989)				
NGC 315	2.493	1.756	21.46	5126
NGC 741	2.447	1.705	21.73	5546
NGC 4839	2.387	1.442	21.59	6955
NGC 7626	2.511	1.561	20.97	7615
3C 40	2.233	0.960	20.92	5426

Table 4. Radio Galaxies from literature, continued.

name	$\log\sigma$	$\log r_\mathrm{e}$ kpc	$<\mu_\mathrm{e}>$	V_r km/s
Ledlow & Owen (1995)+ EFAR/Hypercat				
0039–095B	2.447	0.362	17.69	16 604
0053–015	2.473	1.186	20.46	11 459
0053–016	2.396	0.866	19.57	12 798
0110+152	2.292	1.253	20.96	13 137
0112–000	2.401	0.799	19.63	13 582
0112+084	2.562	1.500	21.35	14 740
0147+360	2.384	0.601	18.57	5227
0306+237	2.396	0.811	19.18	20 122
0431–133	2.430	1.382	21.02	9825
0431–134	2.346	0.714	19.39	10 393
1510+076	2.526	0.455	18.45	12 927
1514+072	2.393	1.664	22.17	10 308
1520+087	2.342	1.497	21.85	10 223
1602+178A	2.328	0.849	20.01	9350
1610+296	2.508	0.814	18.76	9602
2322+143a	2.310	0.550	18.96	13 381
2335+267	2.538	1.349	20.71	9060
Gonzalez-Serrano & Carballo (2000)+ Hypercat				
NGC 507	2.517	1.005	19.72	4621
NGC 708	2.382	1.385	21.58	4498
gin116	2.455	1.021	19.80	9791
NGC 4869	2.299	0.788	19.58	6895
NGC 4874	2.425	1.487	21.22	7428
NGC 6086	2.508	1.181	20.57	9534
NGC 6137	2.47	1.506	20.66	9348

galaxies from Heckman et al. (1985). Among the latter ones, only 7 are supplied with complete photometric information, whereas 5 objects, out of the remaining 27 in the total sample, turn out to belong to dumbbell systems or close pairs. This reduces the usable sample of SHI90 to 22 objects available for FP analysis. In order to derive $<\mu_\mathrm{e}>$ consistently with our definitions (see above formula) we used their isophotal magnitudes V_{25} and the effective radii r_e reported in SH89 (Table 8) and applied a correction of -0.16 (average difference between m_tot and $m_{24.5}$ in our study of RG; Govoni et al. 2000b) to obtain total magnitudes. Then we corrected for the color term $(V-R)$ using the colors from SH89, when available, or assuming $(V-R)=0.55$ in the other cases.

3.2. Additional data for the Fundamental Plane of LzRG

In order to improve the statistics of our analyses, we have searched the literature for additional LzRG that have measurements of velocity dispersion, $<\mu_\mathrm{e}>$ and r_e. We have combined photometric data of LzRGs from the studies of Ledlow & Owen (1995, LO95) and Gonzalez-Serrano & Carballo (2000, GC00) whith the velocity dispersions given by Wegner et al. (1999, EFAR) or by Hypercat.

The cross identification betwen LO95 and EFAR added 17 new LzRGs to our compilation, whereas that between GC00 and Hypercat adds 7 more LzRGs. In both cases, in order to derive $<\mu_\mathrm{e}>$ consistently with our definitions, we used the magnitudes $m_{24.5}$ and the effective radii r_e given in the original papers and applied the same corrections as for the data of SHI90.

In total, the sample of LzRG for which we collected data from the literature consists of 51 objects. The relevant data for these objects are given in Tables 3 and 4. These, together with the sample for which we present new data, leads to a total of 73 LzRG, and represents the largest dataset of photometric and spectroscopic data on Radio Galaxies till now.

3.3. Comparison sample of non-radio elliptical galaxies

In order to compare the FP of LzRGs with that of normal galaxies, we used the sample of radio-quiet early–type galaxies studied by Jørgensen et al. (1996, JFK96). It is by far the richest, still homogeneous sample for which both photometric and kinematic information is available. Previous samples of early type galaxies used to describe the FP (e.g. FA89) have a significantly larger scatter with respect to the data of JFK96. Since the JFK96 sample consists of cluster galaxies, it has also the advantage of the reliability of the distance determination.

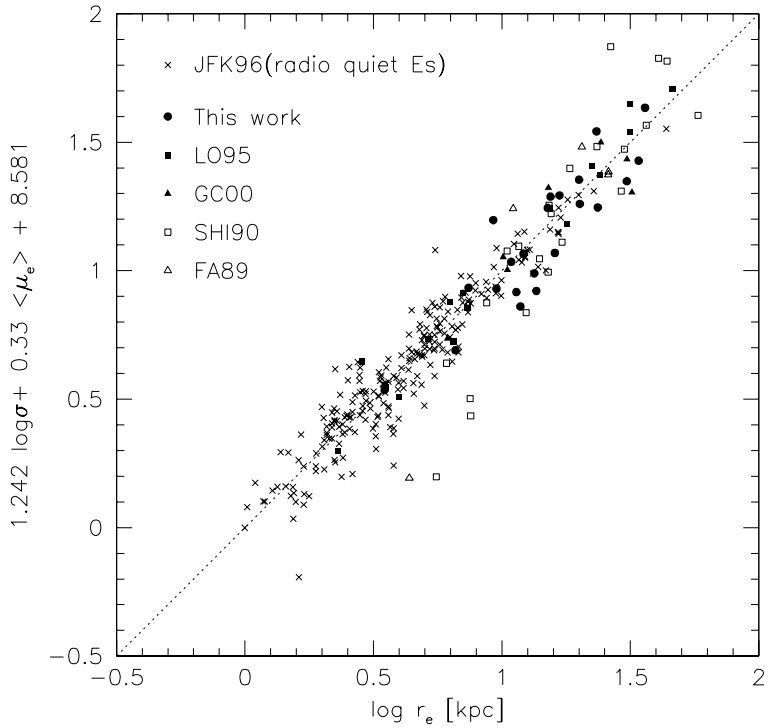

Fig. 2. The Fundamental Plane of various samples of LzRG (see legend and Table 5) and normal (non radio) ellipticals (JFK96), compared with the best fit (dotted line) to the JFK96 data.

Table 5. The FP in R.

Sample	$N_{\rm gal}$	α	β	γ	rms
J (JFK96)	229	1.24 ± 0.04	0.330 ± 0.007	8.58 ± 0.06	0.059
O (This Work)	22	1.36 ± 0.23	0.295 ± 0.031	8.15 ± 0.23	0.071
L (LO95)	17	1.24 ± 0.23	0.311 ± 0.015	8.21 ± 0.18	0.047
G (GC00)	7	2.55 ± 0.74	0.311 ± 0.073	11.37 ± 0.53	0.055
S (SHI90)	22	2.60 ± 0.31	0.161 ± 0.021	8.19 ± 0.26	0.070
F (FA89)	5	2.31 ± 0.48	0.072 ± 0.043	5.86 ± 0.50	0.030
OLG	46	1.58 ± 0.16	0.310 ± 0.015	8.99 ± 0.15	0.063
OLGSF	73	1.92 ± 0.15	0.256 ± 0.013	8.69 ± 0.15	0.082
JOLG	275	1.27 ± 0.04	0.326 ± 0.007	8.56 ± 0.06	0.060
JOLGSF	303	1.35 ± 0.04	0.308 ± 0.007	8.40 ± 0.06	0.069

To compare our data on LzRG with the JFK96 data, we converted their Gunn r photometry to the R band, by means of the average relation $R - r = 0.3$, given in Jørgensen (1994).

4. The Fundamental Plane of radiogalaxies

In order to derive the parameters describing the FP:

$$\log r_{\rm e}^{\rm kpc} = \alpha \log \sigma + \beta <\mu_{\rm e}>_R - \gamma, \quad (1)$$

we minimized the root square of the residuals perpendicular to the plane. This procedure is to be preferred with respect to the classical one (minimizing the root square of the residuals along a given axis) when there are measurement errors in all observed quantities. It is also slightly different from that used by JFK96, which minimizes the sum of the absolute residuals perpendicular to the plane.

In Table 5 the FP coefficients α, β and γ obtained using this fitting procedure for different subsamples of radio and non radio galaxies are reported. Since the adopted fitting procedure does not provide analytical form for the uncertainties of the parameters, we indicate in Table 5 the 1σ uncertainties computed according to the classical formalism and assuming the values of the FP coefficients given in the table.

Each sample in the table is indicated with a capital letter and the fits obtained merging together two or more samples are indicated with sequences of letters, according to the previous correspondence (for instance JO means JFK96+This Work).

We note from Table 5 that, in spite of the slightly different fitting procedure, the FP coefficients we found for the JFK96 sample of radio-quiet galaxies (our comparison sample) are indistinguishable from those given in the original JFK96 paper (see their Eq. (1)). In Fig. 2 we plot all the galaxies in the above described samples, together with our FP fit of non radio ellipticals (JFK96).

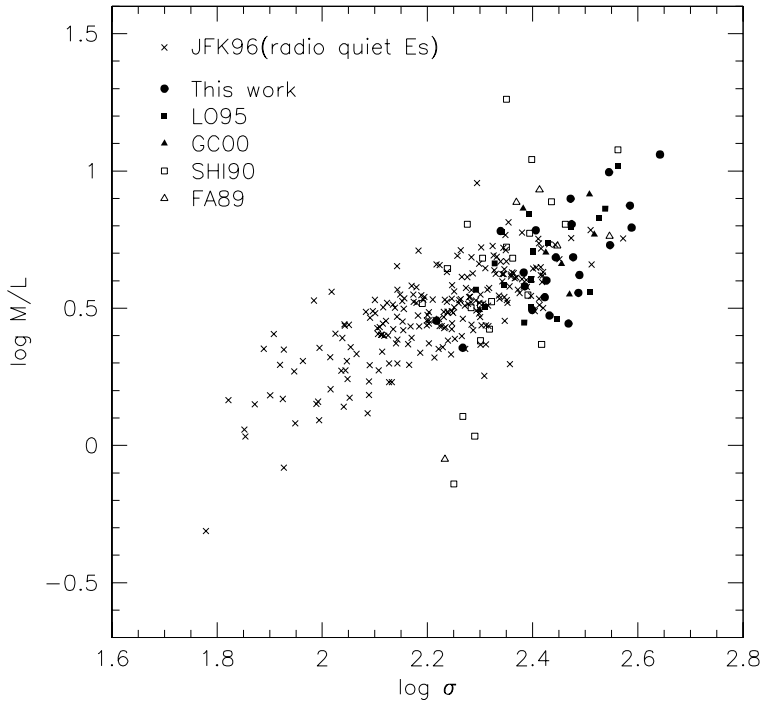

Fig. 3. The M/L ratio versus the velocity dispersion relationship of Radio Galaxies compared with that for early type galaxies (JFK96).

From Table 5 the FP coefficients derived from our sample of 22 radio-galaxies turn out to be consistent (within 1σ of the estimated uncertainties) with those relative to the control sample of non radio galaxies. The same happens for the 17 radio-galaxies in the L095 sample. On the contrary, fitting the SHI90 sample of 22 radio-galaxies yields FP coefficients different (well beyond 3σ) from those relative to the comparison sample. This is likely to be due to the presence of a few outliers in their galaxy sample, as shown in Fig. 2. Finally, given the small size of FA89 and GC00 samples a reliable estimate of the FP can not be derived from them. Nevertheless, we have reported in Table 5 the coefficients resulting from the formal fit of these samples. In the case of the GC00 sample, they are consistent with those relative to the control sample, whereas considerable differences (again caused by the presence of an outlier) come in the case of the FA89 sample.

In Table 5 we also report the fits obtained merging together two or more galaxy samples. Among them, we assume as representative of the global FP of elliptical galaxies, the fit:

$$\log r_{\rm e}^{\rm kpc} = 1.27 \log \sigma + 0.326 <\mu_{\rm e}>_R - 8.56 \qquad (2)$$

which includes the comparison sample (JFK96) and the radio samples from this work(O), from LO95(L) and from GC00(G). This fit allows to extend the FP up to the bright end of the luminosity function of early–type galaxies.

The M/L ratio is a function of the stellar population and dark matter content of galaxies. In Fig. 3 we show the relation between the Mass to Light ratio (M/L) and the velocity dispersion σ. We derived the masses of our galaxies by using the relation $M = 5\, r_{\rm e}\sigma^2/G$ (Bender et al. 1992). This figure indicates that LzRGs follow the same relation found for normal elliptical galaxies. The scatter of the M/L ratio as a function of $\log \sigma$ is $\sim$0.2 dex, similar to that found by JFK96.

5. Conclusions

The main conclusion of this study is that the fundamental plane of radio galaxies, as defined by our collection of data for 73 objects, is consistent with the one defined by normal, non-radio elliptical galaxies. Some recent results on BH demography (Ferrarese & Merrit 2000; Gebhardt et al. 2000) strongly suggest that all galaxies may host a massive BH in the nucleus, and that the BH mass is proportional to the mass of the spheroidal component. This means that, virtually, all ellipticals have the basic ingredient for becoming active. Considering the small amount of gas (few solar masses per year) necessary to sustain the radio emission of even the most powerful radio sources, the activity could be triggered by extremely modest alteration of the status of equilibrium in which galaxies settled soon after they form. According to this view it is therefore not surprising that radio and non radio ellipticals have indistinguishable global properties, irrespective of their nuclear activity. Here, we present one more result supporting this scenario.

Both metallicity effects and age variations have been suggested as the main cause (Faber et al. 1995) of the strong dependence of M/L on σ, that is on the total mass of the galaxy. This relation is consistent with a progressive reddening of the stellar population going from small

to big galaxies (e.g., Prugniel & Simien 1996), but most of dependence remains unexplained. It looks like that ellipticals pass from being baryon dominated to be dark matter dominated with increasing luminosity, with a fine tuning required by the small and basically constant dispersion around the FP.

Acknowledgements. This research made use of Vizier service (Ochsenbein et al. 2000) and of the NASA/IPAC Extragalactic Database (NED) which is operated by the Jet Propulsion Laboratory, California Institute of Technology, under contract with the National Aeronautics and Space Administration. We have made use of the LEDA (`http://leda.univ-lyon1.fr`) and Hypercat database.

Appendix A: Notes on individual galaxies

0055–016 – UGC 595 – 3C 29, this galaxy belongs to the rich cluster A119 and is D26 in the Dressler (1980) list. Smith et al. (1990) measured a velocity dispersion of 199 ± 18 km s^{-1}but recently Wegner et al. (1999) give a value of 253 ± 17 km s^{-1} in better agreement with our measurements.

0131–360 – NGC 612, this galaxy show a strong dust lane along the apparent major axis, our spectrum has been obtained perpendicularly to the dust lane, i.e. along the minor axis of the optical galaxy, no rotation is visible.

0915–118 – 3C 218, Hydra A, a well studied galaxy showing strong [OIII](λ = 5007 Å) emission lines. Heckman et al. (1985) found $\sigma = 308 \pm 38$ km s^{-1}, slightly higher than our measurement 278 ± 78 km s^{-1}.

1107–372 – NGC 3557, we measure a velocity dispersion of 295 ± 7 km s^{-1} and a velocity gradient of $\sim$150 km s^{-1} in the central 5″ in good agreement with data available in Hypercat.

1258–321 – ESO443–G024, this galaxy is in the cluster A3537. Dressler et al. (1991) measured a velocity dispersion of 279 ± 27 km s^{-1} in good agreement with our data.

1333–337 – IC 4296, our value of sigma is lower than the mean value quoted by Hypercat (340 km s^{-1}). The agreement is better with the measure of Franx et al. (1989). From our spectrum, taken at PA = 60° we measure a rotation of $\sim$71 km s^{-1} in agreement with data taken at the same position angle by Saglia et al. (1993).

1400–337 – NGC 5419, our measure is in good agreement with the mean value quoted by Hypercat. The spectrum, taken at PA = 84°, show a maximum rotational velocity of $\sim$90 km s^{-1} over 5″ .

1514+072 – UGC9799, our measure of the velocity dispersion is very close to the mean value of 247 km s^{-1} quoted in Hypercat.

References

Bender, R., Burstein, D., & Faber, S. M. 1992, ApJ, 399, 462
Bertola, F., Bettoni, D., Rusconi, G., & Sedmack, G. 1984, AJ, 89, 356
Busarello, G., Capaccioli, M., Capozziello, S., Longo, G., & Puddu, E. 1997, A&A, 320, 415
Caon, N., Capaccioli, M., & D'Onofrio, M. 1993, MNRAS, 265, 1013
Ciotti, L., Lanzoni, B., & Renzini, A. 1996, MNRAS, 282, 1
Davies, R. L., Efstathiou, G., Fall, S. M., Illingworth, G., & Schechter, P. L. 1983, ApJ, 266, 41
Djorgovski, S., & Davis, M. 1987, ApJ, 313, 59
Dressler, A. 1980, ApJS, 42, 565
Dressler, A., Lynden-Bell, D., Burstein, D., et al. 1987, ApJ, 313, 42
Dressler, A., Faber, S. M., & Burstein, D. 1991, ApJ, 368, 54
Faber, S. M., Wegner, G., Burstein, D., et al. 1989, ApJS, 69, 763 (FA89)
Faber, S. M., Trager, S. C., Gonzales, J. J., & Worthley, G. 1995, in Stellar Populations, IAU Coll. 164, ed. P. C. Van der Kruit, & G. Gilmore (Kluwer Academic Publishers, Dordrecht), 249
Fasano, G., Falomo, R., & Scarpa, R. 1996, MNRAS, 282, 40
Ferrarese, L., & Merrit, D. 2000, ApJ, 539, L9
Fisher, D., Illingworth, G., & Franx, M. 1995, ApJ, 438, 539
Franx, M., Illingworth, G., & Heckman, T. 1989, ApJ, 344, 613
Gebahrdt, K., Bender, R., Bower, G., et al. 2000, ApJ, 359, L13
Ghisellini, G., & Celotti, A. 2001, A&A, 379, L1
Govoni, F., Falomo, R., Fasano, G., & Scarpa, R. 2000a, A&A, 353, 507
Govoni, F., Falomo, R., Fasano, G., & Scarpa, R. 2000b, A&AS, 143, 369
Gonzalez-Serrano, J. I., & Carballo, R. 2000, A&A, 142, 353 (GC00)
Graham, A., Lauer, T. R., Colless, M., & Postman, M. 1996, ApJ, 465, 564
Heckman, T. M., Illingworth, G. D., Miley, G. K., & van Breugel, W. J. M. 1985, ApJ, 299, 41
Jørgensen, I. 1994, PASP, 106, 967
Jørgensen, I., Franx, M., & Kjærgaard, P. 1995, MNRAS, 276, 134
Jørgensen, I., Franx, M., & Kjærgaard, P. 1996, MNRAS, 280, 167 (JFK96)
Ledlow, M. J., & Owen, F. N. 1995, AJ, 110, 1959 (LO95)
Mobasher, B., Guzman, R., Aragon-Salamanca, A., & Zepf, S. 1999, MNRAS, 304, 225
Ochsenbein, F., Bauer, P., & Marcout, J. 2000, A&A, 143, 23
Owen, F. N., & Laing, R. A. 1989, MNRAS, 238, 357
Owen, F. N., & White, R. A. 1991, MNRAS, 249, 164
Pahre, M. A., Djorgovski, S. G., & de Carvalho, R. R. 1995, ApJ, 453, L17
Paturel, G., Andernach, H., Bottinelli, L., et al. 1997, A&AS, 124, 109
Poggianti, B. 1997, A&ASS, 122, 399
Prugniel, Ph., & Simien, F. 1996, A&A, 309, 749
Prugniel, Ph., & Maubon, G. 2000, Dynamics of Galaxies: from the Early Universe to the Present, ASP Conf. Ser., 197, 403
Saglia, R. P., Bender, R., & Dressler, A. 1993, A&A, 279, 75
Sargent, W. L. W., Schechter, P. L., Boksenberg, A., & Shortridge, K. 1977, ApJ, 212, 326
Scarpa, R., & Urry, M. 2001, ApJ, 556, 749
Smith, E. P., & Heckman, T. M. 1989b, ApJ, 341, 658 (SH89)
Smith, E. P., Heckman, T. M., & Illingworth, G. D. 1990, ApJ, 356, 399 (SHI90)
Wegner, G., Colless, M., Saglia, R. P., et al. 1999, MNRAS, 306, 259 (EFAR)